Since January 2020 Elsevier has created a COVID-19 resource centre with free information in English and Mandarin on the novel coronavirus COVID-19. The COVID-19 resource centre is hosted on Elsevier Connect, the company's public news and information website.

Elsevier hereby grants permission to make all its COVID-19-related research that is available on the COVID-19 resource centre - including this research content - immediately available in PubMed Central and other publicly funded repositories, such as the WHO COVID database with rights for unrestricted research re-use and analyses in any form or by any means with acknowledgement of the original source. These permissions are granted for free by Elsevier for as long as the COVID-19 resource centre remains active.

Journal of Controlled Release 342 (2022) 388–399

Contents lists available at ScienceDirect

Journal of Controlled Release

journal homepage: www.elsevier.com/locate/jconrel

The role of nanoparticle format and route of administration on self-amplifying mRNA vaccine potency

Giulia Anderluzzi [a,b,1], Gustavo Lou [a,b,1], Stuart Woods [a], Signe Tandrup Schmidt [a,d], Simona Gallorini [b], Michela Brazzoli [b], Russell Johnson [c], Craig W. Roberts [a], Derek T. O'Hagan [c], Barbara C. Baudner [b,*], Yvonne Perrie [a,*]

[a] Strathclyde Institute of Pharmacy and Biomedical Sciences, University of Strathclyde, 161 Cathedral St., Glasgow G4 0RE, Scotland, UK
[b] GSK, Siena, Italy
[c] GSK, Rockville, MD 9911, USA
[d] Department of Infectious Disease Immunology, Center for Vaccine Research, Statens Serum Institut, Artillerivej 5, 2300 Copenhagen S, Denmark

ARTICLE INFO

Keywords:
Self-amplifying RNA
saRNA
RNA vaccines
Lipid nanoparticles
Polymeric nanoparticles
Solid lipid nanoparticles
Route of administration
Immunogenicity

ABSTRACT

The efficacy of RNA-based vaccines has been recently demonstrated, leading to the use of mRNA-based COVID-19 vaccines. The application of self-amplifying mRNA within these formulations may offer further enhancement to these vaccines, as self-amplifying mRNA replicons enable longer expression kinetics and more potent immune responses compared to non-amplifying mRNAs. To investigate the impact of administration route on RNA-vaccine potency, we investigated the immunogenicity of a self-amplifying mRNA encoding the rabies virus glycoprotein encapsulated in different nanoparticle platforms (solid lipid nanoparticles (SLNs), polymeric nanoparticles (PNPs) and lipid nanoparticles (LNPs)). These were administered via three different routes: intramuscular, intradermal and intranasal. Our studies in a mouse model show that the immunogenicity of our 4 different saRNA vaccine formulations after intramuscular or intradermal administration was initially comparable; however, ionizable LNPs gave higher long-term IgG responses. The clearance of all 4 of the nanoparticle formulations from the intramuscular or intradermal administration site was similar. In contrast, immune responses generated after intranasal was low and coupled with rapid clearance for the administration site, irrespective of the formulation. These results demonstrate that both the administration route and delivery system format dictate self-amplifying RNA vaccine efficacy.

1. Introduction

The role of mRNA vaccines in global healthcare is now well established. mRNA vaccines can be classified into modified and non-modified mRNA and self-amplifying mRNA (saRNA) vaccines. saRNA are developed from the genome of positive-stranded RNA viruses (usually alphaviruses) in which the genes encoding the viral structural proteins are replaced by the gene(s) encoding the antigen(s) of interest. They also contain the alphavirus-based open read frame that encodes four nonstructural proteins (nsP1-4). When expressed, nsP1-4 form RNA-dependent RNA polymerase (RDRP) complexes, which enables self-amplification [1]. As a consequence, saRNA replicons enable longer expression kinetics [2] and significantly more potent immune responses [3] than non-amplifying mRNAs. However, RNAs are polyanionic and susceptible to enzymatic degradation, limiting their entry into cells; therefore, delivery systems are needed. Incorporation of RNA vaccines into nanoparticles provides RNA protection and improved delivery into cells. To date, lipid nanoparticles (LNPs) based on ionizable amino-lipids are the most advanced RNA delivery systems [4], and this technology is deployed in COVID-19 vaccines [5,6].

Previous studies on saRNA-LNPs suggest that the route of administration strongly influences the kinetics and magnitude of antigen expression and the potency of the immune response, though most studies focus on intramuscular (IM) as the preferred way to deliver both mRNA and saRNA vaccines [7–10]. For example, Geall and co-workers demonstrated that the intramuscular injection of a saRNA encoding respiratory syncytial virus fusion protein (RSV-F) either unformulated or formulated within lipid nanoparticles elicited neutralizing antibody

* Corresponding authors.
E-mail address: yvonne.perrie@strath.ac.uk (Y. Perrie).
[1] These authors contributed equally.

https://doi.org/10.1016/j.jconrel.2021.12.008
Received 20 June 2021; Received in revised form 26 November 2021; Accepted 6 December 2021
Available online 10 December 2021
0168-3659/© 2022 Elsevier B.V. All rights reserved.

titers in both mice and rats; however, saRNA-LNPs were significantly more potent than naked saRNA [11]. It has also been reported that LNPs based on either 1,2-dioleoyl-3-trimethylammonium-propane (DOTAP) or dimethyldioctadecylammonium (DDA) and co-formulated with saRNA-HIV-1 Env gp140 induced equivalent IgG antibody responses against the target protein in mice when administered intramuscularly [12]. However, antigen-specific immunity with mRNA can be achieved via several other administration routes, e.g. intravenous, intradermal (ID), subcutaneous (SC), intranodal, and intrasplenic [13]. For example, the immunogenicity of a saRNA vaccine encoding the HIV gp140 surface glycoprotein, formulated in LNPs based on the ionizable lipid DLin-DMA, was tested after administration by a variety of routes, and it was shown to be more effective when administered via the IM route compared with the ID and SC routes. However, the differences between IM and ID groups was not significant [11]. Similarly, IM or ID vaccination with a hemagglutinin (HA)-encoded saRNA vaccine formulated in LNPs resulted in comparable antibody and HA inhibition titers [14]. In a third study, also with an HA-mRNA-LNP vaccine, HAI titers were significantly higher following ID vaccination compared to IM two weeks after the boost, but equivalent at later time points [15].

However, consideration of alternative routes for vaccination may offer opportunities. For example, the derma skin layer is abundant in professional antigen-presenting cells e.g. dendritic dermal cells and Langerhans cells [16] which can enhance encoded antigen transportation to the lymph nodes and induce protective immune responses. Thus, intradermal administration may facilitate lower vaccine doses (dose-sparing), thereby reducing costs (including transport and storage) and expanding the supply chain. Indeed, the potential of dermal non-viral delivery of saRNA vaccines was reported previously [17]; the skin is extremely immune competent, easily accessible and drugs can be administered by means of needle-free devices, thus improving patient compliance, reducing the risk of needle-stick injures and reducing clinical waste. Intranasal (IN) vaccination is another needle-free, noninvasive administration route for vaccines. The nasal cavity is embedded with a high density of dendritic cells that can mediate strong systemic and local immune responses against pathogens [18]. The uptake of nasally administered vaccines is mediated by M cells, which transport particulate antigens to the nasal lymphoid tissue by transcytosis. Nasal vaccination induces both systemic and mucosal immunity in the respiratory and genital tracts by the release of IgA into the nasal passage and intestinal tract. This administration route is adopted by AstraZeneca's FluMist (a live-attenuated influenza virus vaccine approved for human use) and has been investigated for the delivery of an mRNA-based HIV vaccine, with strong systemic and mucosal anti-HIV immune responses as well as cytokine productions being achieved [19].

Whilst both intradermal and intranasal administration offers potential advantages, there is limited understanding of RNA vaccine efficacy when given via these routes compared with the conventional intramuscular route. Therefore, the aim of this study was to compare the efficacy of self-amplifying mRNA vaccines when delivered using 4 different delivery platforms and via the intramuscular, intradermal or intranasal route. Building on our previous studies, where we show that lipid nanoparticles (LNPs), solid lipid nanoparticles (SLNs) and polymeric nanoparticles (PNPs) based on commercially available cationic lipids such as 1,2-dioleoyl-3-trimethylammonium-propane (DOTAP) efficiently deliver self-amplifying mRNA vaccines in mice [20,21], we investigate the role of administration route on the immunogenicity elicited. To compare their performance across different delivery routes, the same formulations were tested across the different routes. An saRNA encoding the rabies virus glycoprotein (RVG) was used, as commercial vaccines can be tested as benchmarks and immunological correlates of protection are well-established [22,23].

2. Materials and methods

2.1. Materials

1,2-dioleoyl-sn-3-phosphoethanolamine (DOPE), dimethyldioctadecylammonium bromide (DDA), 1,2-dioleoyl-3-trimethylammonium-propane (DOTAP) and 1,2-dimyristoyl-sn-glycero-3-phosphoethanolamine-N-[methoxy(polyethylene glycol)-2000] (DMG-PEG2000) were obtained from Avanti Polar Lipids (Alabaster, US). Poly (D, L-lactide-*co*-glycolide) lactide: glycolide (50:50), MW 30,000-60,000, Dimethyl Sulfoxide, Tristearin (Grade II-S, ≥90%), 3 M sodium acetate buffer pH 5.2, Trizma hydrochloride solution 1 M, penicillin-streptomycin, L-glutamine, cholesterol (Chol) and brefeldin A (BFA) were purchased from Sigma (Milan, Italy). RiboGreen RNA assay kit, 1,1'-Dioctadecyl-3,3,3′,3'-Tetramethylindotricarbocyanine Iodide (DiR), Alexa Fluor 488-labeled goat anti-mouse IgG2a Cross-Adsorbed secondary antibody and allophycocyanin (APC) Zenon antibody labelling kit for mouse IgG2a were purchased from Thermo Fisher (Milan, Italy). Dulbecco's Modified Eagle Medium (DMEM), Roswell Park Memorial Institute 1640 medium (RPMI-1640), Hank's balance salt solution (HBSS) trypsin-EDTA (0.25%) and fetal bovine serum (FBS) were obtained from Gibco. PLATELIA Rabies II Kit was obtained from Bio-Rad (Milan, Italy). 100 mM citrate buffer pH 6.0 was purchased from Teknova (Milan, Italy). Live/dead fixable dead cell stain near-IR was purchased from Life Technologies (Milan, Italy). Mouse anti-rabies glycoprotein antibody (clone 24-3F-10) was obtained from Merck (Milan, Italy). 10× Perm/Wash buffer and Cytofix/Cytoperm were obtained from BD Biosciences (San Jose, CA, USA). Anti-mouse PE-CF594-conjugated CD8, V421-conjugated CD44, PE-conjugated TNF-α and BV786-conjugated IFN-γ and FITC-conjugated CD107a monoclonal antibodies and anti-mouse Ig, κ/negative control compensation particles set were obtained from BD Horizon (San Jose, CA, USA). Anti-mouse BV510-conjugated CD4, APC-conjugated CD3 and PE-Cy5-conjugated IL-2 monoclonal antibodies and RBC lysis buffer were purchased from Biolegend (San Diego, CA, USA). Anti-mouse PE-Cy7-conjugated IL-17, CD28 and CD3 monoclonal antibodies were purchased from ePharmingen (San Jose, CA, USA). The rabies peptide pool containing peptides of 15-mers with 11 amino acid overlap was obtained from Genescript (Piscataway NJ, USA). Rabipur is a trademark of the GSK group of companies.

2.2. Synthesis of self-amplifying RNA (saRNA)

A self-amplifying RNA (saRNA) vaccine encoding the rabies virus glycoprotein (RVG) was synthesized as previously described [11]. In brief, DNA plasmids encoding the RVG-saRNA were constructed using standard molecular techniques. Plasmids were amplified in *Escherichia coli* and purified using Qiagen Plasmid Maxi kits (Qiagen, Germantown, MD, USA). DNA was linearized following the 3′ end of saRNA sequence by restriction digest. Linearized DNA templates were transcribed into RNA using a MEGAscript T7 kit (Life Technologies, Carlsbad, CA, MA, USA) and purified by LiCl precipitation. RNA was then capped using the Vaccinia Capping system (New England BioLabs, Ipswich, MA, USA) and purified by LiCl precipitation before formulation.

2.3. Formulation and characterization of LNPs, PNPs and SLNs

DOTAP-based formulations were prepared and characterized as previously described [20,21]. In essence, DOTAP LNPs were composed of DOPE, DOTAP and DMG-PEG2000 at 49:49:2 M ratio; DOTAP PNPs were composed of PLGA (lactide:glycolide 50:50) and DOTAP 1:1 *w*/w and DOTAP-SLNs were composed of tristearin, DOTAP (1:1 *w*/w) and 2 mol% of DMG-PEG2000. These formulations were produced by a microfluidic mixer (Precision NanoSystems Inc., Vancouver, Canada) using a flow rate ratio of 3:1 (for LNPs and SLNs) or 1:1 (for PNPs) and flow rate of 15 mL/min. Benchmark iLNPs described by Geall et al. [11] were produced in the same manner as cLNPs. Lipids/polymers dissolved

in an organic solvent (methanol, DMSO or ethanol for LNPs, PNPs and SLNs respectively) and an aqueous phase (100 mM citrate buffer pH 6.0 for LNPs, 10 mM TRIS pH 7.4 for SLNs or 100 mM acetate buffer pH 6 for PNPs) containing RVG-saRNA at 8:1 N:P (N in DOTAP and P in saRNA) were injected simultaneously in the micromixer. All formulations were dialyzed against 10 mM TRIS pH 7.4 and characterized in terms of hydrodynamic size (*Z*-average), polydispersity index (PDI) and zeta potential by dynamic light scattering (DLS) in a Zetasizer Nano ZS (Malvern, UK) at 0.1 mg/mL at 25 °C. The saRNA encapsulation efficiency (saRNA E.E.) was quantified by RiboGreen assay following manufacturer instructions. Fluorescence was measured at excitation and emission wavelength of 485 and 528 nm. saRNA E.E. was calculated as $(F_T - F_0)/F_T$ where F_T and F_0 are the amount of saRNA quantified in presence and absence of 1% Triton X-100 respectively. Prior to in vivo administration, formulations were diluted to dosing concentration with the addition of NaCl 20 mM in the dilution buffer to maintain isotonicity. Low levels of endotoxins (<10 EU/mL) and sterility conditions were preserved across all formulations.

2.4. Immunization studies

All animal studies were ethically reviewed and carried out in accordance with European Directive 2010/63/EEC and the GSK policy on the Care, Welfare and Treatment of Animals. Experiments were performed at the GSK Animal Facility in Siena, Italy, in compliance with the relevant guidelines (Italian Legislative Decree n. 26/14) and the institutional policies of GSK. The animal protocol was approved by the Animal Welfare Body of GSK Vaccines, Siena, Italy, and by the Italian Ministry of Health (Approval number "AWB 2015 01", CPR/2015/01). Groups of 10 female BALB/c mice (Charles Rivers) aged 6–8 weeks and weighing about 20–25 g were immunized with RVG-saRNA formulated in either LNPs, PNPs or SLNs on days 0 and 28 either intramuscularly (IM), intradermally (ID) or intranasally (IN). Mice received 0.15 μg of saRNA-RVG in 50 μL when administered IM, 0.15 μg of RVG-saRNA in 20 μL when administered ID or 1.5 μg in 50 μL when given IN. Three further groups were vaccinated with the commercial vaccine Rabipur (a trademark of the GSK group of companies) either IM (2% of the human dose (HD), 50 μL), ID (2% HD, 20 μL) or IN (5% HD, 50 μL). A higher dose was given IN due to the expected reduced efficacy of this route.

2.5. Quantification of antibody titers

Sera from individual mice were collected four weeks after the first vaccination (day 28) and two weeks after the second vaccination (day 42) and combined in five pools of two mice each. Total anti-RVG IgG titers were quantified with the PLATELIA RABIES II Kit Ad Usum Veterinarium [22] following manufacturer instructions.

2.6. Intracellular cytokine staining (ICS) in splenocytes

Spleens from 3 randomly selected mice from each experimental group were collected on day 42 (two weeks after the second vaccination). Single cell suspensions were obtained as described elsewhere [24]. Cells were then incubated with RBC lysis buffer (2 mL) at 4 °C for 2 min, resuspended in complete RPMI (cRPMI) and passed again through cell strainers. Cells were counted in a Vi-CELL XR cell counter (Beckman Coulter) and $1.5 \cdot 10^6$ splenocytes/well were cultured in round-bottomed 96-well plates. Splenocytes were stimulated with an RVG-derived peptide pool library (2.5 μg/mL) consisting of 15-mers with 11 amino acid overlaps and anti-CD28 (2 μg/mL) in presence of brefeldin A (5 μg/mL) for 4 h at 37 °C. Cells were also stimulated with anti-CD3 (1 μg/mL) plus anti-CD28 (2 μg/mL) or anti-CD28 alone as positive and negative controls respectively. Samples were then stained with a live/dead fixable near-IR dead cell stain kit, then fixed and permeabilized with Cytofix/Cytoperm and subsequently stained with the following antibodies in Perm/Wash Buffer: APC-conjugated anti-CD3, BV510-conjugated anti-CD4, PE-CF594-conjugated anti-CD8, BV785-conjugated anti-IFN-γ, PE-Cy5-conjugated anti-IL-2, anti-BV605-conjugated TNF-α and PE-Cy7-conjugated anti-IL-17. Samples were acquired in an LSR II flow cytometer (BD Biosciences, San Jose, CA, USA) and analyzed in FlowJo Software (BD BioScience, San Jose, CA, USA). Antigen-specific CD4+ T cell subsets were identified based on the combination of secreted cytokines as follows: Th1 (IFN-γ + IL-2+ TNF-α+; IFN-γ + IL-2+; IFN-γ + TNF-α+; IFN-γ+); Th0 (IL-2+ TNF-α+; IL-2+; TNF-α+). The frequency of antigen-specific CD8+ T cells was identified based on the combination of IFN-γ+, IL-2+ and TNF-α + .

2.7. Lung processing and quantification of T-cell derived cytokines

Lung tissue was completely dissociated with Gentlemax Dissociator (Milteny Biotec, Bologna, Italy). Briefly, lung tissue was digested in Hank's Balanced Salt Solution containing calcium and magnesium in the presence of collagenase D (2 mg/mL) and DNAse I (80 units/mL) (both from Sigma (Milan, Italy)) for 30 min at 37 °C, and then homogenized until obtaining a single-cell suspension. Then, 2×10^6 cells were seeded into 96-well U-bottom plates stained with Live/Dead Near InfraRed, fixed and permeabilized, plated with anti-CD28 mAb (2 μg/mL) and anti-CD107a FITC (5 μg/mL). As a positive control, cells were added to wells coated with anti-CD3 mAb (1 μg/mL). Moreover, as ex vivo restimulation, cells were stimulated for 4 h with an RVG peptide pool at 2.5 μg/mL. Brefeldin A (5 μg/mL) was added to each condition for the last 4 h. For flow cytometry analysis, cells were incubated with anti-CD16/CD32 Fc block and further stained with anti-CD3-APC, anti-CD4-BV510, anti-CD8 PE, anti–IFN-γ BV785, anti–IL-2 PE-Cy5.5, anti–TNF-α PE, and anti–CD44 V421, anti-IL-17 PE as intracellular markers. Samples acquisition and analysis were performed as described above.

2.8. Biodistribution studies

Biodistribution studies were conducted under the regulations of the Directive 2010/63/EU. All protocols were subjected to ethical review and were carried out in a designated establishment in the animal facility. All work was carried out under a project license with approval from the University of Strathclyde Ethical Review Board. In order to track their biodistribution in vivo, LNPs, PNPs and SLNs were co-formulated with the lipophilic fluorescent dye 1,1'-Dioctadecyl-3,3,3′,3'-Tetramethylindotricarbocyanine Iodide (DiR) as previously described [25]. Groups of five 6–8-week-old female BALB/c mice injected with either LNPs, PNPs or SLNs (25 μg, containing 1 μg of DiR dye) intramuscularly (50 μL in the right thigh), intradermally (20 μL in the dorsum) or intranasally (10 μL per nostril). Mice imaging was carried out using an IVIS Spectrum (Perkin Elmer, Beaconsfield, UK) using Living Image software for data capture and analysis. The presence of DiR was detected using an excitation wavelength of 710 nm and an emission filter of 780 nm. A medium binning and f/stop of 2 was used and acquisition time was determined for each image with auto-exposure settings. Mice were anaesthetized for imaging using 3% IsoflurFane. Anesthesia was maintained during imaging at 1% Isoflurane. Images were taken before administration of formulations and after 4, 24, 48, 72, 144 and 240 h post injection. The total flux (p/s) was calculated at the injection site (region of interest) for each mouse and normalised by dividing each time point by the value at 4 h time point as it was the highest in each group. This was considered as 100%,

2.9. Statistical analysis

Statistical analysis of T cell responses and biodistribution experiments was performed by one-way analysis of variance (ANOVA) followed Tukey's honest significance test. Statistical analysis of IgG titers was performed by Kruskal-Wallis followed by Dunn's test. *P* values below 0.05 (*) were considered significant. All analyses were done in

A)

Nanoparticle Composition	
SLNs	DOTAP, tristearin and DMG-PEG2000
PNPs	DOTAP, PLGA and DMG-PEG2000
cLNPs	DOTAP, DOPE and DMG-PEG2000
iLNPs	Ionizable lipid, DOPE and DMG-PEG2000

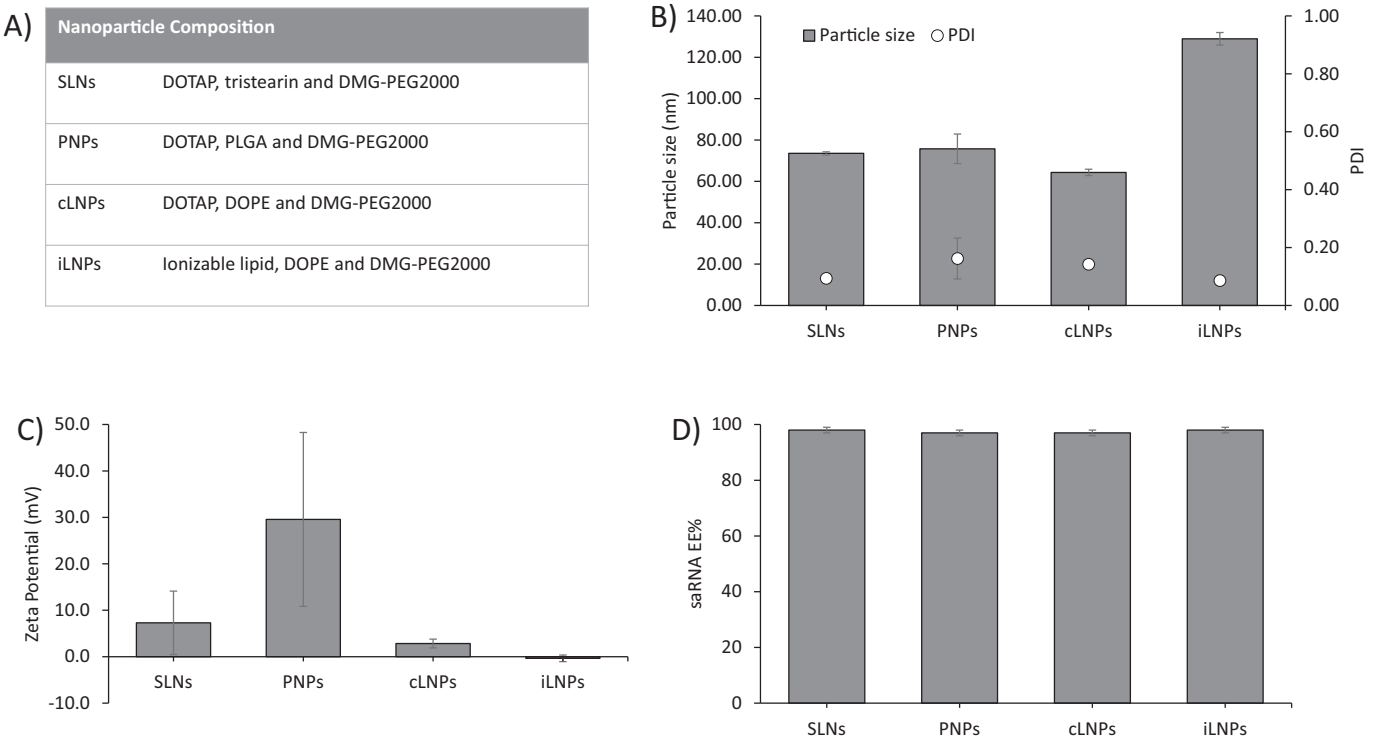

Fig. 1. Physicochemical characterization of saRNA formulations. SLNs, PNPs, cLNPs and iLNPs were prepared as outlined in (A) and characterized in terms of B) particles size (d.nm) and polydispersity index (PDI), C) zeta-potential (mV) and D) encapsulation efficiency (EE%). Results are represented as mean ± SD of two different batches used for first and second vaccination respectively.

GraphPad Prism 7.0.

3. Results and discussion

3.1. Characterization of saRNA-nanoparticles

We have previously reported the microfluidic production of several nanoparticles based on the commercially available cationic lipid DOTAP [20,21]. The use of microfluidics in the manufacturing process supports process driven size control and scale-independent production [26,27]. Within this study, we selected three different nanoparticle formats (LNPs, PNPs and SLNs) to further investigate the role of administration route on self-amplifying RNA vaccine performance (Fig. 1). Whilst cationic LNPs tend to display bilayer-like structures [28], PNPs consisting of a polymer core and SLNs have a lipid monolayer surrounding the polymer core [29]. These formulations were selected based on previous studies which demonstrated these formulations were capable of associating with cells, inducing antigen expression in vitro and protecting SaRNA against enzymatic degradation [20,21]. The same formulations were used across the different delivery routes to allow direct comparison. Our particles were from 65 to 135 nm in size, with low PDI (<0.2), near neutral zeta potential, except for the PNPs which were cationic, and high saRNA encapsulation efficiency (>95%) (Fig. 1 B–D). Particle size has been suggested to play a role in the immunogenicity of mRNA vaccines in mice [30]. However, more recent studies suggest this may only be a feature of small animal studies [31]; a retrospective analysis of mRNA LNP vaccine in vivo studies revealed a relationship between LNP particle size and immunogenicity in mice using LNPs of various compositions. Nevertheless, whilst small diameter LNPs were substantially less immunogenic in mice, all particle sizes tested yielded a robust immune response in non-human primates [31].

Table 1
Routes of administration and vaccine (RVG-saRNA or Rabipur) doses used to immunize BALB/c mice.

Vaccine	Route of administration	Dose	Dose volume
saRNA (formulated in LNPs, PNPs or SLNs)	IM	0.15 μg	50 μL
	ID	0.15 μg	20 μL
	IN	1.5 μg	50 μL
Rabipur	IM	2% HD	50 μL
	ID	2% HD	20 μL
	IN	5% HD	50 μL

saRNA: self-amplifying RNA; LNPs: lipid nanoparticles, PNPs: polymeric nanoparticles; SLNs: solid-lipid nanoparticles; IM: intramuscular; ID: intradermal; IN: intranasal; HD: human dose.

3.2. Immunogenicity of RVG-saRNA formulated in LNPs, PNPs and SLNs following intramuscular, intradermal and intranasal administration

mRNA and saRNA vaccines are commonly administered IM or ID [16,32] and mRNA vaccines are now approved for IM administration. However, there are very few pre-clinical studies that have systematically compared the immunogenicity of RNA vaccines delivered by different routes of administration. Therefore, using the formulations outlined in Fig. 1, we assessed the impact of administration route on saRNA vaccine efficacy when delivered using the different nanoparticle formats. Mice were vaccinated twice, four weeks apart, with RVG-saRNA formulated in either SLNs, PNPs, cLNPs or benchmark iLNPs [33] and delivered intramuscularly (IM), intradermally (ID) or intranasally (IN). Control groups were vaccinated with Rabipur, an inactivated rabies virus vaccine. The selected doses were based on our previous findings with these

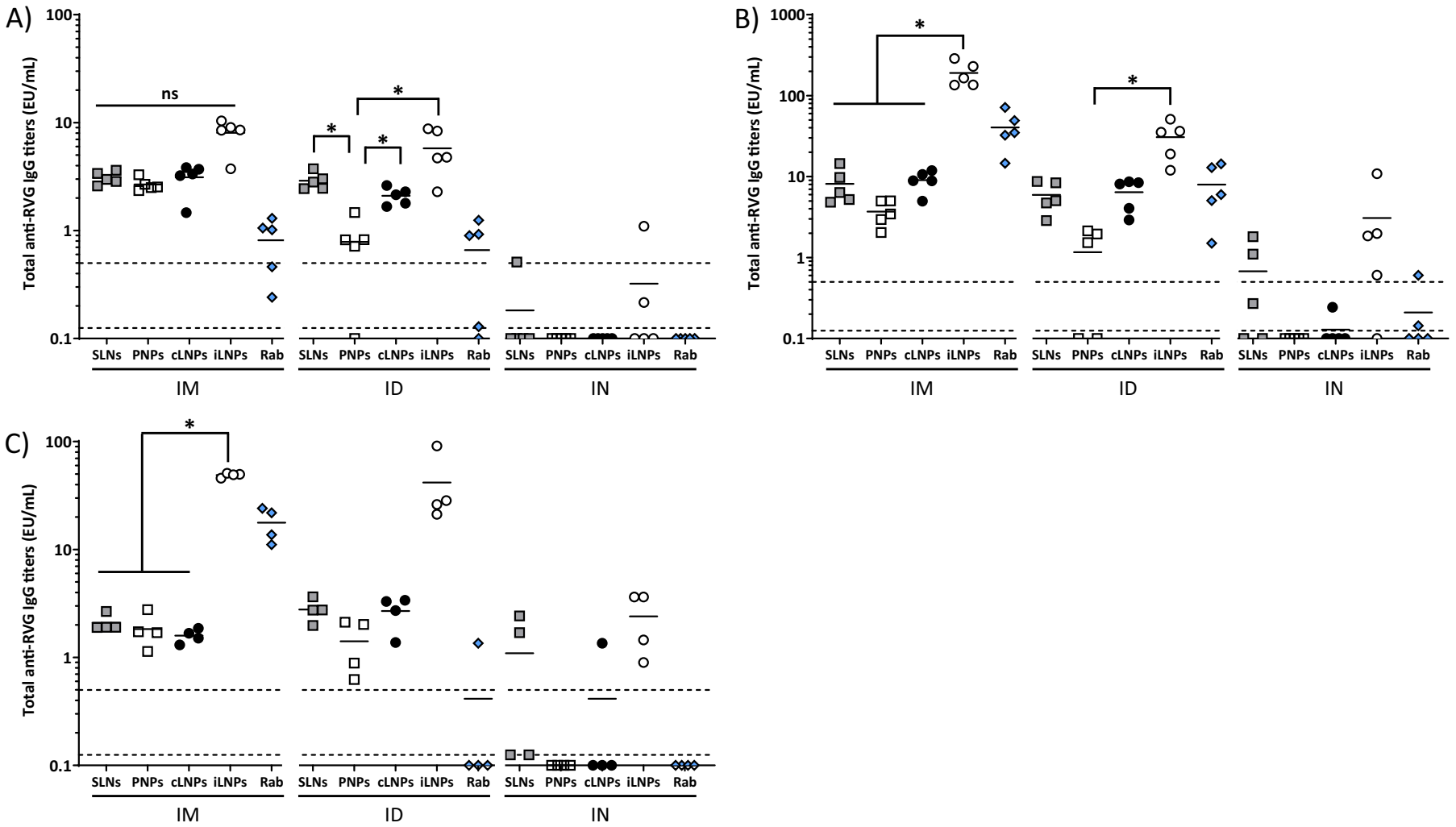

Fig. 2. Immunogenicity of RVG-saRNA loaded SLNs, PNPs and LNPs. Humoral immune responses elicited by RVG-saRNA formulated in either DOTAP-based SLNs, PNPs or LNPs following intramuscular (IM, 0.15 μg), intradermal (ID, 0.15 μg) or intranasal (IN, 1.5 μg) administration in mice. Mice were also immunized with benchmark iLNPs [11] or 2% (IM and ID) or 5% (IN) of the human dose of Rabipur. Mice were vaccinated four weeks apart and total anti-RVG IgG titers were quantified four weeks after the first vaccination (A), two weeks after the second vaccination (B) and 10 weeks after the second vaccination (C). Markers depict measurements from pools of 2 mice each. The solid lines represent the geometric mean titer of each group ($n = 4–5$). Dotted lines at 0.5 and 0.125 EU/mL correspond to the correlate of protection and limit of quantification, respectively.

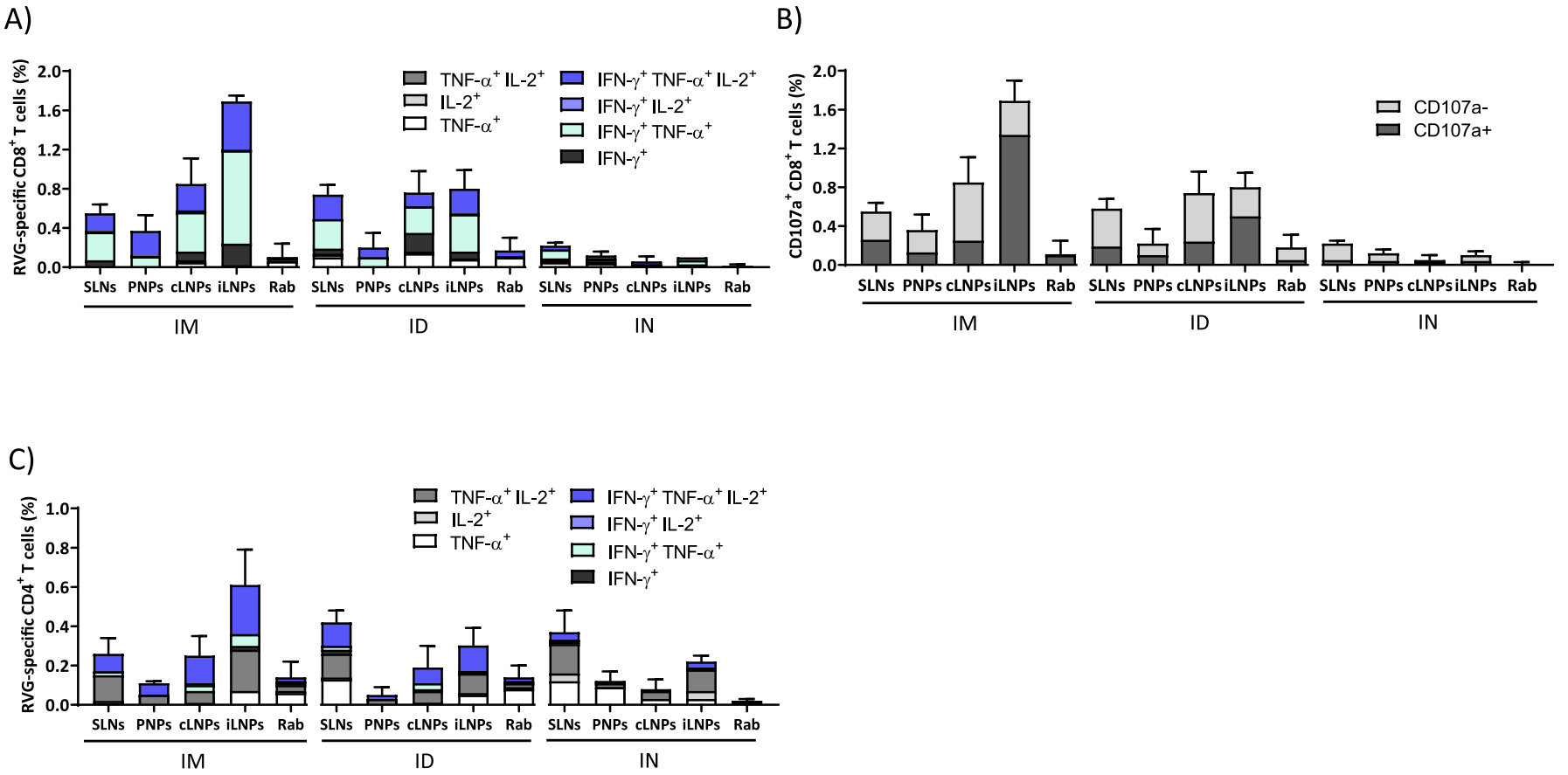

Fig. 3. Cellular immune response elicited by RVG-saRNA loaded nanoparticles after IM, ID or IN administration. Splenic CD8+ and CD4+ T cell responses elicited by RVG-saRNA formulated in either DOTAP-based SLNs, PNPs or LNPs following intramuscular (IM, 0.15 μg), intradermal (ID, 0.15 μg) or intranasal (IN, 1.5 μg) administration in mice. Mice were also immunized with benchmark iLNPs [11] and either 2% (IM and ID) or 5% (IN) of the human dose of Rabipur. Splenocytes were collected two weeks after the second vaccination and re-stimulated in vitro with an RVG peptide pool. A) Frequencies of cytokine-producing CD8+ T cells. B) Frequencies of CD107+ CD8+ T cells. C) Frequencies of CD4+ T cells expressed as Th1 and Th0 according to the cytokines expressed. Results are represented as mean ± SD of three samples. Refer to Fig. S1 in the supplemental material for the gating strategy.

delivery systems [20,21] (Table 1).

IgG responses were measured prior to immunization, 4 weeks post first injection (day 28), 2 weeks after the second injection (day 42) and 10 weeks after the second injection (day 98). No anti-RVG IgGs were detected in mice sera prior to immunization (data not shown). Four weeks after the first injection, there was no significant difference between the IgG responses promoted by the 4 different nanoparticle formulations (SLNs, PNPs, cLNPs, iLNPs) when administered IM. All 4 nanoparticle formulations induced strong antigen-specific IgG titers above the correlate of protection of 0.5 EU/mL and these responses were significantly ($p < 0.05$) higher than the control vaccine (Rabipur) (Fig. 2A). When the mice were dosed ID, generally a similar response profile was shown with antigen-specific IgG titers above the correlate of protection of 0.5 EU/mL. However, PNPs promoted significantly lower responses compared to the SLNs, cLNPs and the iLNPs benchmark (Fig. 2A). After IN administration there were no notable IgG responses measured, with IgG titers below the limit of quantification in all but three samples, despite mice receiving a 10 folder higher dose via this route (Fig. 2A). Overall, at this time point, IM and ID administration with the various nanoparticle formulations gave comparable responses, with the exception of PLPs given ID. Administration via the IN route failed to induce notable responses irrespective of the formulation.

After the second vaccination, the immune responses elicited generally increased approximately 3-fold after both IM and ID vaccination with the exception of the PNPs, where the booster dose had little effect on the immune response (Fig. 2B). Comparing between the nanoparticle formulations, after an IM booster injection, iLNPs produced significantly ($p < 0.05$) higher IgG responses compared to the three DOTAP formulations (SLNs, PNPs, cLNPs). When a second dose was administered ID, there was no difference between SLNs, cLNPs and iLNPs. However, PNPs promoted significantly ($p < 0.05$) lower IgG responses compared to iLNPs (Fig. 2B). Again, the immune responses induced upon IN immunization were significantly weaker compared to IM or ID immunization for all of the formulations tested with only the iLNPs promoting an average response above the correlate of protection (Fig. 2B). Overall, after the second immunization, iLNPs administered IM promoted the strongest IgG responses (Fig. 2B).

This pattern of immune response was also seen 10 weeks post second immunization, demonstrating the ability of these nanoparticle formulations to induce persistent humoral immunity above the correlate of protection (Fig. 2C). When administered IM, iLNPs continued to promote significantly ($p < 0.05$) higher IgG titers compared to the SLNs, PNPs and cLNP formulations. When administered ID, there was no significant difference between the 4 different nanoparticle formulations but a similar trend of higher responses from iLNPs was seen (Fig. 2C). Comparing between the routes of administration at this timepoint, IM and ID gave similar response profiles yet when administered IN, only the iLNPs promoted a notable IgG response with all responses above the correlate of protection (Fig. 2C).

The results in Fig. 2 are in line with recent studies of Blakney and coworkers, who reported equivalent antibody production in mice vaccinated either IM or ID with saRNA formulated within poly(CBA-*co*-4-amino-1-butanol) (ABOL)-based nanoparticles at different doses [34]. Although all formulations elicited antibodies titers above the level of protective response to rabies vaccination reported by WHO [35], LNPs and SLNs were generally more potent than PNPs two weeks after the second vaccination, and overall iLNPs gave the highest long term response via both the IM and ID routes. In our previous studies [20,21], these formulations did not notably differ in terms of in vitro antigen expression nor in vivo antibody titers after IM injection. The combination of nanoparticle formulation and route of administration may result in different cellular kinetic or pharmacokinetic properties e.g. endosomal disruption potential and/or release kinetics of saRNA. When administered intranasally, all saRNA-nanoparticle formulations were poorly immunogenic, despite animals receiving a 10-fold higher dose of RVG-saRNA compared to IM or ID (1.5 μg vs 0.15 μg). The weak immunogenicity of candidates upon IN vaccination may be due to multiple factors. For example, rapid clearance from the administration site and/or the acidic, protease-rich and reductase-rich environment of the mucosae [36] may induce potential loss of activity and functionality of saRNA.

To study the immune response profiles further, cytokine responses were also measured. The saRNA-nanoparticles formulations induced multifunctional RVG-specific cellular immune responses two weeks after the second vaccination (Fig. 3). Generally, LNPs injected either IM or ID induced the highest frequencies of cytokines-producing RVG-specific splenic CD4+ and CD8+ T cells (Fig. 3). Similar to the IgG profiles, the frequencies of cytokine-producing CD8+ T cells in mice that received iLNPs were greater than the other formulations after IM (Fig. 3A). When administered ID, their profiles are similar for the SLNs, cLNPs and iLNPs whilst the responses induced by the PNPs are low (Fig. 3A). The majority of RVG-specific CD8+ T cells expressed IFN-γ in combination with TNF-α and/or IL-2, irrespective of the route of administration, and this is generally associated with a mature effector phenotype. The strong proliferation of CD8+ T cells triggered by saRNA vaccines is consistent with previous studies which demonstrated that saRNA formulated with LNPs injected IM induced antigen expression within muscle cells and its consequent presentation to APCs, suggesting cross-priming as the prevalent mechanism for CD8+ T-cell response activation by saRNA vaccines [37]. Similar to the IgG profiles, the frequencies of cytokine expression were low in mice vaccinated IN (Fig. 3A). A similar trend was observed in the expression of the degranulation marker CD107a (Fig. 3B), whose expression correlates with the cytotoxic activity of CD8+ T cells in vivo [38,39]. In mice vaccinated IM, the frequencies of CD107a + CD8+ T cells were highest with the iLNPs, whilst after ID, the responses induced by iLNPs reduced and were comparable with the cLNPs and SLNs (Fig. 3B). After IN administration, only negligible percentages of CD107a + CD8+ T cells were quantified (<0.1%, Fig. 3B). With respect to the CD4+ T cell responses, again a similar profile of responses is seen (Fig. 3C); after IM injection iLNPs promote the highest responses in mice, whilst after ID these responses reduce and are similar to SLNs and cLNPs (Fig. 3C). However, SLNs administered via the IN route promoted responses in line with the responses promoted by SLNs given IM and ID (Fig. 3C).

The CD4+ T cells proliferation induced by RNA vaccines is likely to be related to the rapid activation of lymphatic cells. For example, Liang and colleagues [15] showed that mRNA-LNPs administered either intradermal or intramuscular in rhesus macaques specifically targeted APCs located both at the injection site and in draining lymph nodes, leading to antigen translation and upregulation of type I IFN-inducible genes. This rapid innate immunity induced priming of antigen-specific CD4+ T cells and generation of vaccine-specific immunity solely in the draining lymph nodes. Similar observations were also reported elsewhere [40]. The relative frequency of CD8+ and CD4+ T cells quantified for each formulation and route of administration (Fig. 3) was also consistent with the production of antibodies reported in Fig. 2. A combination of Th0 (IL-2+/TNF-α+, TNF-α+, or IL-2+) and Th1 (IFN-γ + alone or in combination with IL-2+ and/or TNF-α+) phenotypes were observed in CD4+ T-cells 2 weeks after the second immunization in all groups (Fig. 3C). Interestingly, ID injection of SLNs resulted in the highest frequencies of polyfunctional antigen-specific CD4+ T cells. The potential of ID vaccination has been widely established in many clinical trials, although results are not always consistent among different vaccines. For example, dermal injection of lower doses of a virus-inactivated influenza vaccine resulted in equivalent immunogenicity to the standard dose delivered intramuscularly [41]. With respect to the rabies virus, post-exposure IM or ID vaccination with Rabipur resulted in similar neutralizing antibody titers in humans but ID was slightly lower compared to IM in a pre-exposure prophylaxis regime [42]. Conversely, with the hepatitis B vaccine, the benefit of dose-sparing was not fully evident [43].

Intranasally administered vaccines have the potential to induce

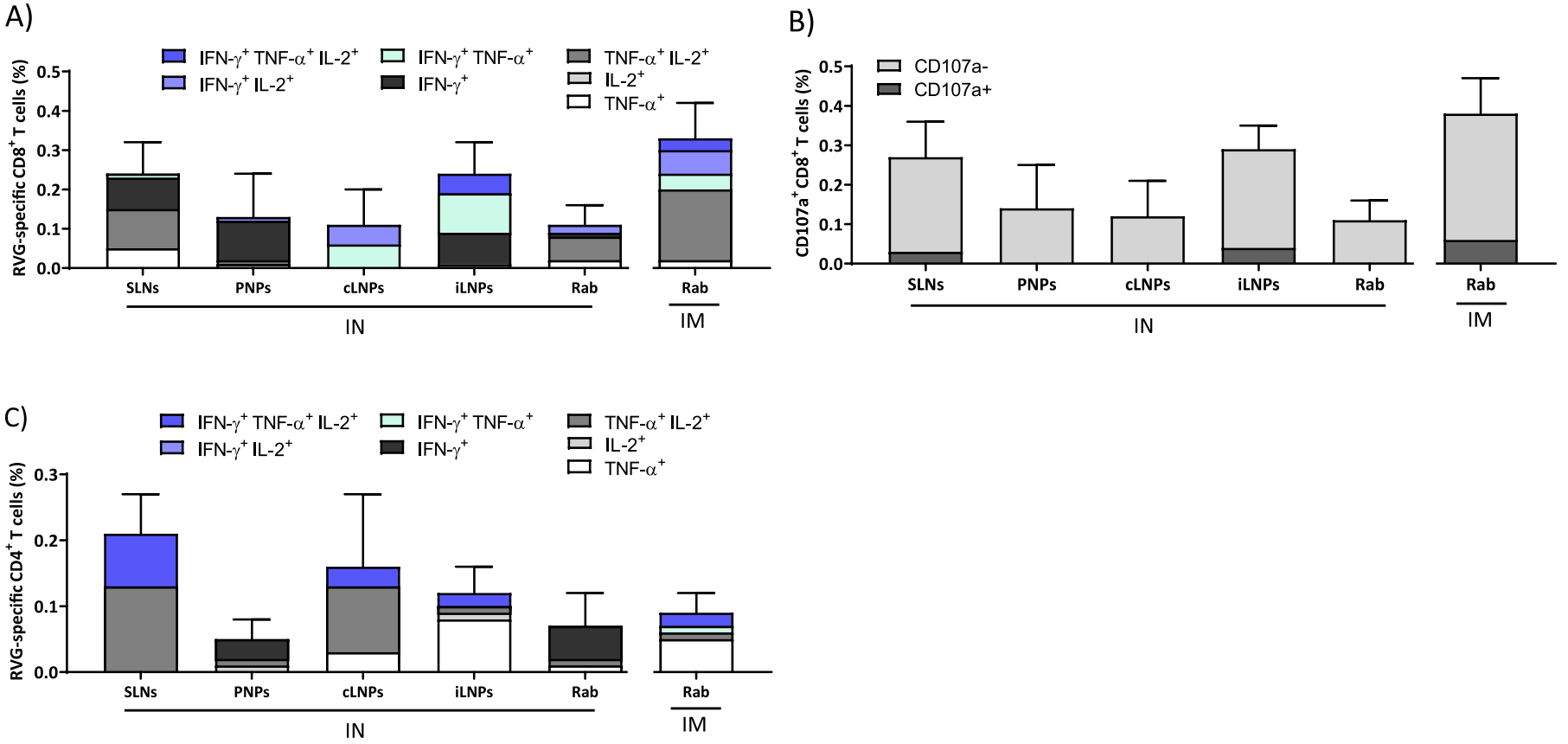

Fig. 4. Lung CD8+ and CD4+ T cell responses following intranasal vaccination. Lung cells were collected two weeks after the second vaccination and re-stimulated in vitro with an RVG peptide pool. A) Frequencies of cytokine-producing CD8+ T cells. B) Frequencies of CD107+ CD8+ T cells. C) Frequencies of CD4+ T cells expressed as Th1 and Th0 according to the cytokines expressed. Results are represented as mean ± SD of three samples. Refer to Fig. S2 in the supplemental material for the gating strategy.

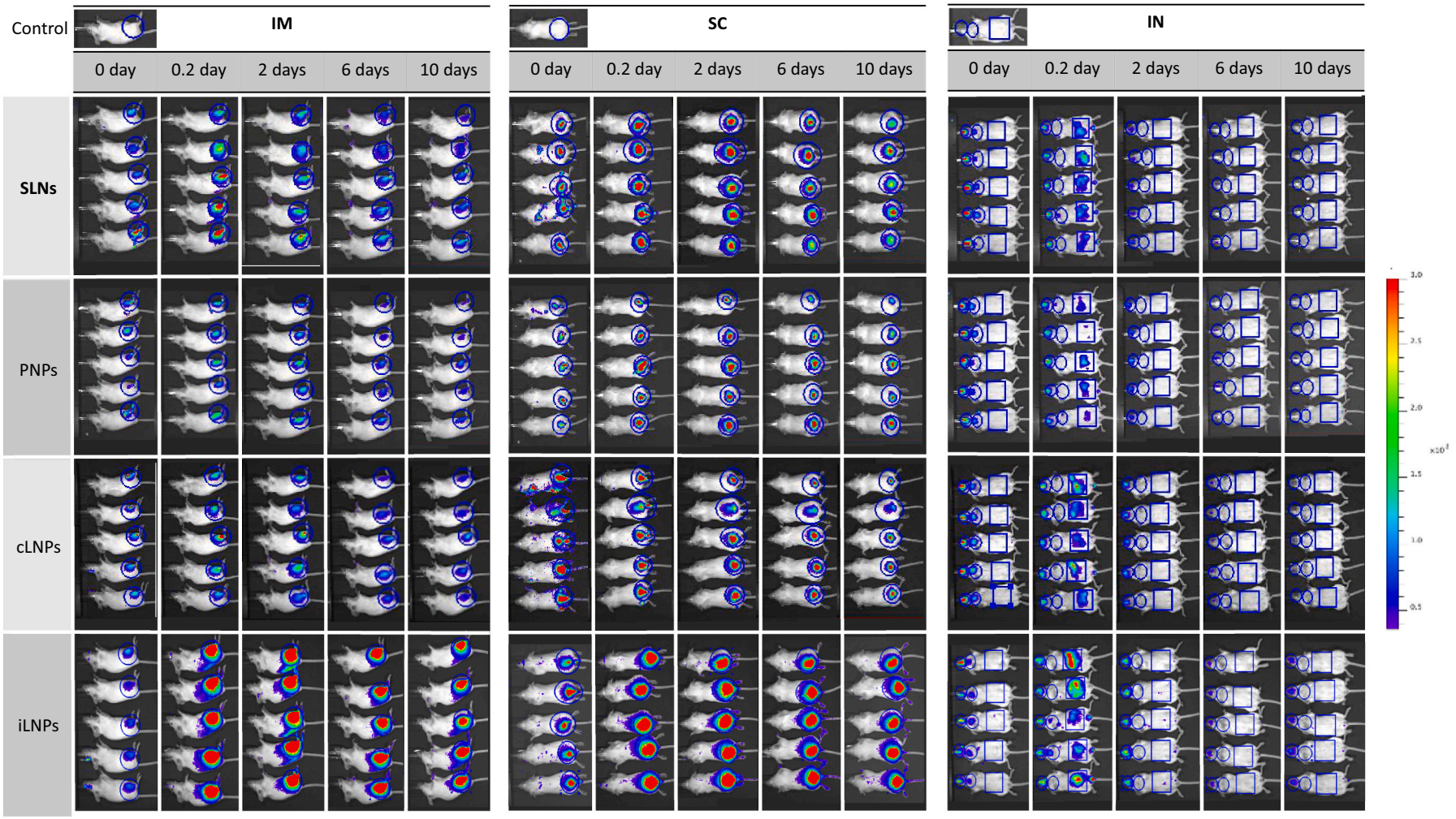

Fig. 5. Biodistribution of RVG-saRNA loaded SLNs, PNPs and LNPs in a mouse model. Representative IVIS images of groups of 5 BALB/c mice injected with either saRNA-SLNs, saRNA-PNPs or saRNA-LNPs by the intramuscular (IM), intradermal (ID) or intranasal (IN) route at selected time points. Mice received 25 μg of nanoparticles, corresponding to the administration of 1 μg of saRNA. The total flux was calculated in the regions of interest highlighted in blue. Scale of fluorescence is reported. Refer to Fig. S3 in the supplementary for enlarged images of mice at all time points over 10 days p.i. (For interpretation of the references to colour in this figure legend, the reader is referred to the web version of this article.)

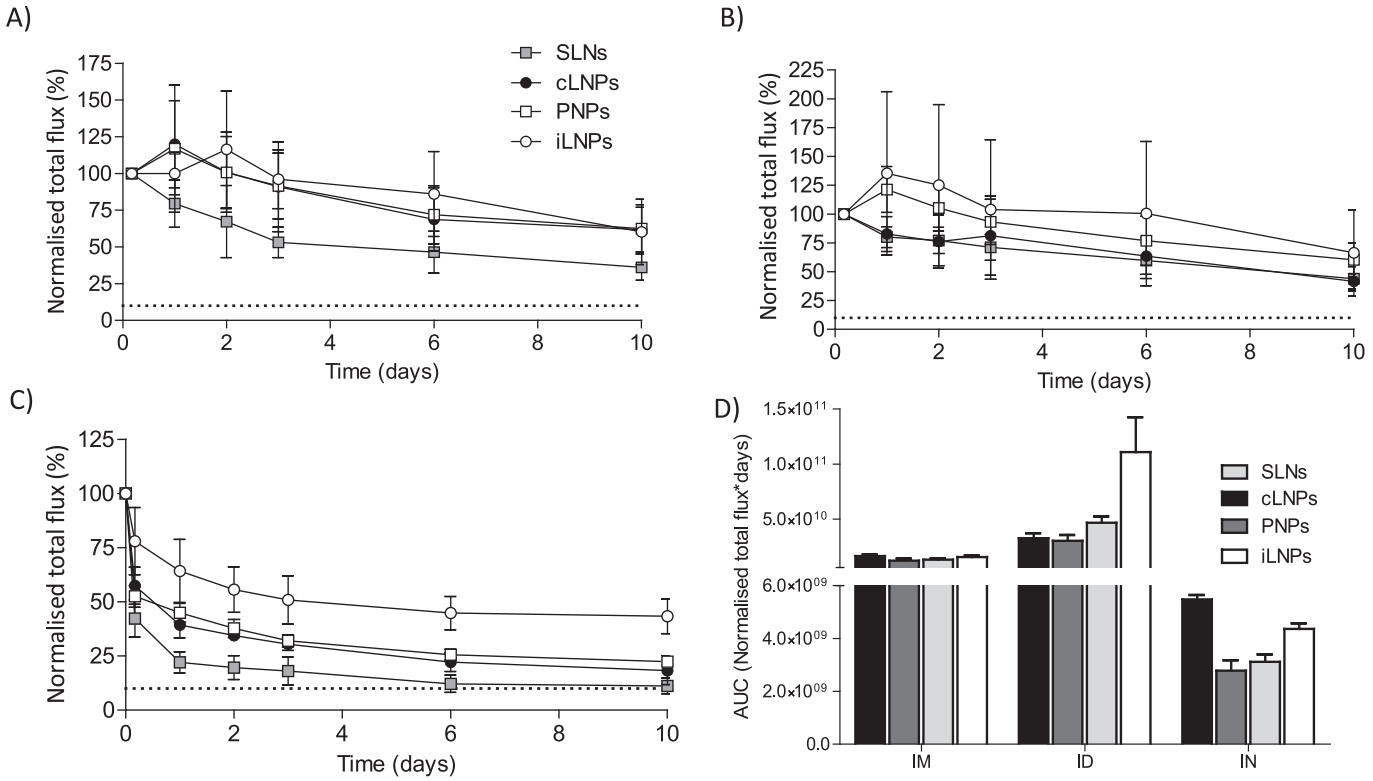

Fig. 6. Pharmacokinetic profile at the site of injection of RVG-saRNA loaded SLNs, PNPs and LNPs. Pharmacokinetic profile at the site of injection of either saRNA-SLNs, saRNA-PNPs or saRNA-LNPs following A) intramuscular, B) intradermal or C) intranasal administration. Mice received 25 μg of nanoparticles, corresponding to the administration of 1 μg of saRNA. A naive mouse was used as a negative control. D) Calculated areas under the curve at the site of injection for saRNA encapsulating LNPs, PNPs and SLNs administered by intramuscular (IM), intradermal (ID) or intranasal (IN) route. The total flux was normalised by dividing each time point by the value at 4 h time point as it was the highest in each group. This was considered as 100%Dotted line represents the background value. Results are represented as mean ± SD of five animals per group.

persistent lung effector T cells, which could significantly benefit host immunity against respiratory pathogens [24]. Therefore, to further investigate this, we performed a T cell assay in lung cells from mice immunized IN. iLNPs and SLNs elicited a higher frequency of RVG-specific CD8+ T cells compared to LNPs, PNPs and Rabipur when administered IN. Furthermore, both formulations gave comparable responses to Rabipur administered IM (Fig. 4A). Interestingly, the quality of CD8+ T cell responses in the lungs varied among tested formulations: SLNs and PNPs induced polyfunctional CD8+ IFN-γ + and TNF-α+/IL-2+ cells, while those elicited by cLNPs were IFN-γ/TNF-α + and IFN-γ+/IL-2+ and those elicited by iLNPs were γ/TNF-α+, IFN-γ+/IL-2+ and IFN-γ + (Fig. 4A). However, the majority of RVG-specific CD8+ T-cells were CD107a- (Fig. 4B) irrespective of the nanoparticle formulation used, which correspond to a non-cytotoxic profile. Regarding CD4+ T cells, the frequencies of RVG-specific cells were comparable between SLNs, cLNPs and iLNPs groups (around 0.2%); however, again the profiles were different with the iLNPs promoting more TNF-α + cells (Fig. 4C). As observed in splenic CD4+ T-cells, cell profile was a combination of Th0/Th1 phenotypes, with SLNs inducing a higher frequency of Th1 cells than LNPs and PNPs respectively (Fig. 4C). These differences in T cell responses may be attributed to differences in the nanoparticle chemical composition and/or mRNA delivery profile. For example, fatty acids are known to modulate cytokines secretion from activated T cells and the effect is dependent on both the saturation degree and length of fatty acid [44,45]. In particular, it was reported that saturated fatty acids induced significantly higher release of pro-inflammatory cytokines in T cells than their unsaturated counterparts, possibly due to increased formation of free radicals, diacyl glycerol and activation of protein kinase C [46].

3.3. *Biodistribution of saRNA-SLNs, PNPs and LNPs after intramuscular, intradermal and intranasal administration*

Several studies have suggested that the administration route of mRNA vaccines strongly influences the kinetics of antigen expression [47]. For example, in a study conducted with mRNA encoding luciferase formulated in LNPs, the half-life of antigen expression in mice was ranked in the order of intradermal > > intramuscular > intraperitoneal and subcutaneous > > intratracheal > intravenous [47]. Although antigen expression, biodistribution and immunogenicity are expected to be closely related, a defined correlation remains unclear. Indeed, we have previously shown that both cLNPs and iLNPs are retained at the injection site following intramuscular injection for up to 10 days [21]. Here, we compared the pharmacokinetics of saRNA-SLNs, PNPs and LNPs administered via IM, ID or IN to further understand the importance of the delivery route for effective mRNA vaccines.

When considering the biodistribution of the different nanoparticle formulations (Figs. 5 and 6), full body images of mice that received saRNA-nanoparticles via intramuscular or intradermal injection showed that the signal was mainly concentrated at the site of injection (Fig. 5). Long-term retention of all four nanoparticle formulations at the injection site was also observed after both IM (Fig. 6A) and ID (Fig. 6B) administration, with the area under the curve (AUC; calculated using the trapezoidal method) confirming that the drainage profile of the nanoparticles was comparable (Fig. 6D). With respect to IN vaccinated groups, whole body images showed poor retention of all nanoparticles (Fig. 5); most of the administered dose was detected in the throat and stomach at 4 h post administration (Fig. 5) suggesting that part of the vaccine dose had been rapidly swallowed and cleared a few hours after administration, irrespective of the nanoparticle format (Fig. 6C and D).

The rapid clearance of the nanoparticles from the administration site after IN vaccination correlated with the weaker humoral and cellular immune response observed. This may result from ineffective interactions between the nanoparticles and mucosal tissue upon administration due to a lack of muco-adhesive/ muco-penetrating excipients within the nanoparticle formulations. The presence of muco-adhesive or muco-penetrating polymers (e.g. poly(acrylic acid) (PAA), alginate, cellulose derivatives, chitosan, poloxamers and poly(ethylene glycol) (PEG)) on the surface of particles can enhance the concentration of therapeutics delivered to the mucus mesh [48]. Furthermore, the weak potency of vaccines administered IN may also be linked to the unavoidable limitation of the animal model used; intranasal vaccination in small animals may trigger inhalation and ingestion of vaccine antigens, which consequently affects vaccine dosage [49].

By comparing the retention of formulations at the injection site, we did not observe notable differences in clearance between the four saRNA-nanoparticle formulations from either the IM or ID administration, despite the formulations inducing different humoral and cellular responses (Figs. 2 and 3). This suggests that other factors may contribute to the immunogenicity of SaRNA vaccines. These findings are in agreement with previous investigations which showed poor correlation between pharmacokinetics and immunogenicity [30]. Accumulation and trafficking of immune cells transporting the encoded antigen to the draining lymph nodes as well as the mode of antigen delivery to lymphoid tissue might also be involved in the immunostimulatory mechanism of mRNA and saRNA vaccines [40]. The slow clearance of the nanoparticles from the injection site could be due to active uptake by host cells via association with endogenous ligands (e.g. ApoE) and recognition by scavenger receptors and the low-density lipoprotein receptor [50]. ApoE easily associates with the surface of neutral lipid-based particles, resulting in enhanced ApoE-mediated cellular uptake [51]. As these receptors are ubiquitously expressed in all nucleated cells [52], this active targeting could augment nanoparticle retention at the injection site.

4. Conclusions

In this study, we demonstrate that the immunogenicity of our saRNA vaccines for a given delivery route was affected by the format of the nanoparticles. saRNA encapsulated within SLNs and LNPs tending to be more potent than PNPs after administration via the intramuscular or intradermal route and immune responses from these routes were similar. The clearance of all four saRNA nanoparticle formulations from either the IM or ID administration site was also similar. In contrast, immune responses generated after intranasal administration was low (despite receiving a 10-fold higher dose) and coupled with rapid clearance for the administration site irrespective of the formulation, suggesting that further optimization of these systems for this route is required.

Funding

This work was funded by the European Commission Project Leveraging Pharmaceutical Sciences and Structural Biology Training to Develop 21st Century Vaccines (H2020-MSCA-ITN-2015 grant agreement 675370). Independent Research Fund Denmark, grant no. 7026-00027B (STS).

Declaration of Competing Interest

G.A. and G.L. participated to the European Marie Curie PHA-ST-TRAIN-VAC PhD project at the University of Strathclyde (Glasgow, UK) in collaboration with GSK (Siena, Italy); the project was co-sponsored between the University of Strathclyde and GlaxoSmithKline Biologicals S.A. Y.P., S.T.S., C.W.R. and S.W. declare no conflict of interest. S.G, M.B., R.J., D.T.O. and B.C.B are employees of the GSK group of companies. All the authors declare that they have no other relevant affiliations or financial interest in conflict with the subject matter or materials discussed in the manuscript.

Acknowledgements

We wish to thank the saRNA Vaccine Platform Team at GSK Rockville. We also thank the staff at the Animal Research Center and at the Flow-Cy-TOF Core Facility at GSK Siena and the Biological Procedures Unit at the University of Strathclyde for technical assistance.

Appendix A. Supplementary data

Supplementary data to this article can be found online at https://doi.org/10.1016/j.jconrel.2021.12.008.

References

[1] C. Iavarone, D.T. O'hagan, D. Yu, N.F. Delahaye, J.B. Ulmer, Mechanism of action of mRNA-based vaccines, Expert Rev. Vaccines. 16 (2017) 871–881, https://doi.org/10.1080/14760584.2017.1355245.
[2] H. Huysmans, Z. Zhong, J. De Temmerman, B.L. Mui, Y.K. Tam, S. Mc Cafferty, A. Gitsels, D. Vanrompay, N.N. Sanders, Expression kinetics and innate immune response after electroporation and LNP-mediated delivery of a self-amplifying mRNA in the skin, Mol. Ther. - Nucleic Acids. 17 (2019) 867–878, https://doi.org/10.1016/j.omtn.2019.08.001.
[3] A.B. Vogel, L. Lambert, E. Kinnear, D. Busse, S. Erbar, K.C. Reuter, L. Wicke, M. Perkovic, T. Beissert, H. Haas, S.T. Reece, U. Sahin, J.S. Tregoning, Self-amplifying RNA vaccines give equivalent protection against influenza to mRNA vaccines but at much lower doses, Mol. Ther. 26 (2018) 446–455, https://doi.org/10.1016/j.ymthe.2017.11.017.
[4] G. Maruggi, C. Zhang, J. Li, J.B. Ulmer, D. Yu, mRNA as a transformative technology for vaccine development to control infectious diseases, Mol. Ther. 27 (2019) 757–772, https://doi.org/10.1016/j.ymthe.2019.01.020.
[5] P.F. McKay, K. Hu, A.K. Blakney, K. Samnuan, J.C. Brown, R. Penn, J. Zhou, C. R. Bouton, P. Rogers, K. Polra, P.J.C. Lin, C. Barbosa, Y.K. Tam, W.S. Barclay, R. J. Shattock, Self-amplifying RNA SARS-CoV-2 lipid nanoparticle vaccine candidate induces high neutralizing antibody titers in mice, Nat. Commun. 11 (2020) 3523, https://doi.org/10.1038/s41467-020-17409-9.
[6] A.K. Blakney, S. Ip, A.J. Geall, An update on self-amplifying mRNA vaccine development, Vaccines. 9 (2021) 97, https://doi.org/10.3390/vaccines9020097.
[7] J. Lutz, S. Lazzaro, M. Habbeddine, K.E. Schmidt, P. Baumhof, B.L. Mui, Y.K. Tam, T.D. Madden, M.J. Hope, R. Heidenreich, M. Fotin-Mleczek, Unmodified mRNA in LNPs constitutes a competitive technology for prophylactic vaccines, Npj Vaccines. 2 (2017) 29, https://doi.org/10.1038/s41541-017-0032-6.
[8] L.A. Brito, M. Chan, C.A. Shaw, A. Hekele, T. Carsillo, M. Schaefer, J. Archer, A. Seubert, G.R. Otten, C.W. Beard, A.K. Dey, A. Lilja, N.M. Valiante, P.W. Mason, C.W. Mandl, S.W. Barnett, P.R. Dormitzer, J.B. Ulmer, M. Singh, D.T. O'Hagan, A. J. Geall, A cationic Nanoemulsion for the delivery of next-generation RNA vaccines, Mol. Ther. 22 (2014) 2118–2129, https://doi.org/10.1038/mt.2014.133.
[9] J.M. Richner, S. Himansu, K.A. Dowd, S.L. Butler, V. Salazar, J.M. Fox, J. G. Julander, W.W. Tang, S. Shresta, T.C. Pierson, G. Ciaramella, M.S. Diamond, Modified mRNA vaccines protect against Zika virus infection, Cell. 168 (2017) 1114–1125.e10, https://doi.org/10.1016/j.cell.2017.02.017.
[10] A. Hekele, S. Bertholet, J. Archer, D.G. Gibson, G. Palladino, L.A. Brito, G.R. Otten, M. Brazzoli, S. Buccato, A. Bonci, D. Casini, D. Maione, Z.-Q. Qi, J.E. Gill, N. C. Caiazza, J. Urano, B. Hubby, G.F. Gao, Y. Shu, E. De Gregorio, C.W. Mandl, P. W. Mason, E.C. Settembre, J.B. Ulmer, J. Craig Venter, P.R. Dormitzer, R. Rappuoli, A.J. Geall, Rapidly produced SAM ® vaccine against H7N9 influenza is immunogenic in mice, Emerg. Microbes Infect. 2 (2013) 1–7, https://doi.org/10.1038/emi.2013.54.
[11] A.J. Geall, A. Verma, G.R. Otten, C.A. Shaw, A. Hekele, K. Banerjee, Y. Cu, C. W. Beard, L.A. Brito, T. Krucker, D.T. O'Hagan, M. Singh, P.W. Mason, N. M. Valiante, P.R. Dormitzer, S.W. Barnett, R. Rappuoli, J.B. Ulmer, C.W. Mandl, Nonviral delivery of self-amplifying RNA vaccines, Proc. Natl. Acad. Sci. 109 (2012) 14604–14609, https://doi.org/10.1073/pnas.1209367109.
[12] A.K. Blakney, P.F. McKay, B.I. Yus, Y. Aldon, R.J. Shattock, Inside out: optimization of lipid nanoparticle formulations for exterior complexation and in vivo delivery of saRNA, Gene Ther. 26 (2019) 363–372, https://doi.org/10.1038/s41434-019-0095-2.
[13] J.B. Ulmer, P.W. Mason, A. Geall, C.W. Mandl, RNA-based vaccines, Vaccine. 30 (2012) 4414–4418, https://doi.org/10.1016/j.vaccine.2012.04.060.
[14] R. Goswami, D. Chatzikleanthous, G. Lou, F. Giusti, A. Bonci, M. Taccone, M. Brazzoli, S. Gallorini, I. Ferlenghi, F. Berti, D.T. O'Hagan, C. Pergola, B. C. Baudner, R. Adamo, Mannosylation of LNP results in improved potency for self-amplifying RNA (SAM) vaccines, ACS Infect. Dis. 5 (2019) 1546–1558, https://doi.org/10.1021/acsinfecdis.9b00084.
[15] F. Liang, G. Lindgren, A. Lin, E.A. Thompson, S. Ols, J. Röhss, S. John, K. Hassett, O. Yuzhakov, K. Bahl, L.A. Brito, H. Salter, G. Ciaramella, K. Loré, Efficient targeting and activation of antigen-presenting cells in vivo after modified mRNA vaccine administration in Rhesus Macaques, Mol. Ther. 25 (2017) 2635–2647, https://doi.org/10.1016/j.ymthe.2017.08.006.

[16] N. Pardi, M.J. Hogan, F.W. Porter, D. Weissman, mRNA vaccines — a new era in vaccinology, Nat. Rev. Drug Discov. 17 (2018) 261–279, https://doi.org/10.1038/nrd.2017.243.
[17] A. Selmi, F. Vascotto, K. Kautz-Neu, Ö. Türeci, U. Sahin, E. von Stebut, M. Diken, S. Kreiter, Uptake of synthetic naked RNA by skin-resident dendritic cells via macropinocytosis allows antigen expression and induction of T-cell responses in mice, Cancer Immunol. Immunother. 65 (2016) 1075–1083, https://doi.org/10.1007/s00262-016-1869-7.
[18] S. Gallorini, D.T. O'Hagan, B.C. Baudner, Concepts in Mucosal Immunity and Mucosal Vaccines, in: Mucosal Deliv. Biopharm., Springer US, Boston, MA, 2014, pp. 3–33, https://doi.org/10.1007/978-1-4614-9524-6_1.
[19] M. Li, M. Zhao, Y. Fu, Y. Li, T. Gong, Z. Zhang, X. Sun, Enhanced intranasal delivery of mRNA vaccine by overcoming the nasal epithelial barrier via intra- and paracellular pathways, J. Control. Release 228 (2016) 9–19, https://doi.org/10.1016/j.jconrel.2016.02.043.
[20] G. Anderluzzi, G. Lou, S. Gallorini, M. Brazzoli, R. Johnson, D.T. O'Hagan, B. C. Baudner, Y. Perrie, Investigating the impact of delivery system design on the efficacy of self-amplifying RNA vaccines, Vaccines. 8 (2020) 212, https://doi.org/10.3390/vaccines8020212.
[21] G. Lou, G. Anderluzzi, S.T. Schmidt, S. Woods, S. Gallorini, M. Brazzoli, F. Giusti, I. Ferlenghi, R.N. Johnson, C.W. Roberts, D.T. O'Hagan, B.C. Baudner, Y. Perrie, Delivery of self-amplifying mRNA vaccines by cationic lipid nanoparticles: the impact of cationic lipid selection, J. Control. Release 325 (2020) 370–379, https://doi.org/10.1016/j.jconrel.2020.06.027.
[22] M. Feyssaguet, L. Dacheux, L. Audry, A. Compoint, J.L. Morize, I. Blanchard, H. Bourhy, Multicenter comparative study of a new ELISA, PLATELIATM RABIES II, for the detection and titration of anti-rabies glycoprotein antibodies and comparison with the rapid fluorescent focus inhibition test (RFFIT) on human samples from vaccinated and non-vacc, Vaccine. 25 (2007) 2244–2251, https://doi.org/10.1016/j.vaccine.2006.12.012.
[23] L. Stantj, M. Pavlinj, P. Hostnik, S. Levinik-Stezinar, Zaletel-Kragelj, Vaccination against rabies and protective antibodies - comparison of ELISA and fluorescent antibody virus neutralization (FAVN) assays, Vet. Arh. 76 (2006) 281–289.
[24] S. Gallorini, M. Taccone, A. Bonci, F. Nardelli, D. Casini, A. Bonificio, S. Kommareddy, S. Bertholet, D.T. O'Hagan, B.C. Baudner, Sublingual immunization with a subunit influenza vaccine elicits comparable systemic immune response as intramuscular immunization, but also induces local IgA and TH17 responses, Vaccine. 32 (2014) 2382–2388, https://doi.org/10.1016/j.vaccine.2013.12.043.
[25] D. Chatzikleanthous, S.T. Schmidt, G. Buffi, I. Paciello, R. Cunliffe, F. Carboni, M. R. Romano, D.T. O'Hagan, U. D'Oro, S. Woods, C.W. Roberts, Y. Perrie, R. Adamo, Design of a novel vaccine nanotechnology-based delivery system comprising CpGODN-protein conjugate anchored to liposomes, J. Control. Release 323 (2020) 125–137, https://doi.org/10.1016/j.jconrel.2020.04.001.
[26] C.B. Roces, G. Lou, N. Jain, S. Abraham, A. Thomas, G.W. Halbert, Y. Perrie, Manufacturing considerations for the development of lipid nanoparticles using microfluidics, Pharmaceutics. 12 (2020) 1095, https://doi.org/10.3390/pharmaceutics12111095.
[27] G. Anderluzzi, S.T. Schmidt, R. Cunliffe, S. Woods, C.W. Roberts, D. Veggi, I. Ferlenghi, D.T. O'Hagan, B.C. Baudner, Y. Perrie, Rational design of adjuvants for subunit vaccines: the format of cationic adjuvants affects the induction of antigen-specific antibody responses, J. Control. Release 330 (2021) 933–944, https://doi.org/10.1016/j.jconrel.2020.10.066.
[28] J.A. Kulkarni, M.M. Darjuan, J.E. Mercer, S. Chen, R. Van Der Meel, J.L. Thewalt, Y.Y.C. Tam, P.R. Cullis, On the formation and morphology of lipid nanoparticles containing Ionizable cationic lipids and siRNA, ACS Nano 12 (2018) 4787–4795, https://doi.org/10.1021/acsnano.8b01516.
[29] J. Ghitman, E.I. Biru, R. Stan, H. Iovu, Review of hybrid PLGA nanoparticles: future of smart drug delivery and theranostics medicine, Mater. Des. 193 (2020), 108805, https://doi.org/10.1016/j.matdes.2020.108805.
[30] K.J. Hassett, K.E. Benenato, E. Jacquinet, A. Lee, A. Woods, O. Yuzhakov, S. Himansu, J. Deterling, B.M. Geilich, T. Ketova, C. Mihai, A. Lynn, I. McFadyen, M.J. Moore, J.J. Senn, M.G. Stanton, Ö. Almarsson, G. Ciaramella, L.A. Brito, Optimization of lipid nanoparticles for intramuscular administration of mRNA vaccines, Mol. Ther. - Nucleic Acids. 15 (2019) 1–11, https://doi.org/10.1016/j.omtn.2019.01.013.
[31] K.J. Hassett, J. Higgins, A. Woods, B. Levy, Y. Xia, C.J. Hsiao, E. Acosta, Ö. Almarsson, M.J. Moore, L.A. Brito, Impact of lipid nanoparticle size on mRNA vaccine immunogenicity, J. Control. Release 335 (2021) 237–246, https://doi.org/10.1016/j.jconrel.2021.05.021.
[32] P.S. Kowalski, A. Rudra, L. Miao, D.G. Anderson, Delivering the messenger: advances in technologies for therapeutic mRNA delivery, Mol. Ther. 27 (2019) 710–728, https://doi.org/10.1016/j.ymthe.2019.02.012.
[33] P.R. Cullis, M.J. Hope, Lipid nanoparticle systems for enabling gene therapies, Mol. Ther. 25 (2017) 1467–1475, https://doi.org/10.1016/j.ymthe.2017.03.013.
[34] A.K. Blakney, Y. Zhu, P.F. McKay, C.R. Bouton, J. Yeow, J. Tang, K. Hu, K. Samnuan, C.L. Grigsby, R.J. Shattock, M.M. Stevens, Big is beautiful: enhanced saRNA delivery and immunogenicity by a higher molecular weight, bioreducible, cationic polymer, ACS Nano 14 (2020) 5711–5727, https://doi.org/10.1021/acsnano.0c00326.
[35] S.A. Plotkin, Vaccines: correlates of vaccine-induced immunity, Clin. Infect. Dis. 47 (2008) 401–409, https://doi.org/10.1086/589862.
[36] V. Bourganis, O. Kammona, A. Alexopoulos, C. Kiparissides, Recent advances in carrier mediated nose-to-brain delivery of pharmaceutics, Eur. J. Pharm. Biopharm. 128 (2018) 337–362, https://doi.org/10.1016/j.ejpb.2018.05.009.
[37] S. Lazzaro, C. Giovani, S. Mangiavacchi, D. Magini, D. Maione, B. Baudner, A. J. Geall, E. De Gregorio, U. D'Oro, C. Buonsanti, CD8 T-cell priming upon mRNA vaccination is restricted to bone-marrow-derived antigen-presenting cells and may involve antigen transfer from myocytes, Immunology. 146 (2015) 312–326, https://doi.org/10.1111/imm.12505.
[38] L. Zaritskaya, M.R. Shurin, T.J. Sayers, A.M. Malyguine, New flow cytometric assays for monitoring cell-mediated cytotoxicity, Expert Rev. Vaccines. 9 (2010) 601–616, https://doi.org/10.1586/erv.10.49.
[39] E. Aktas, U.C. Kucuksezer, S. Bilgic, G. Erten, G. Deniz, Relationship between CD107a expression and cytotoxic activity, Cell. Immunol. 254 (2009) 149–154, https://doi.org/10.1016/j.cellimm.2008.08.007.
[40] K.E. Lindsay, S.M. Bhosle, C. Zurla, J. Beyersdorf, K.A. Rogers, D. Vanover, P. Xiao, M. Araínga, L.M. Shirreff, B. Pitard, P. Baumhof, F. Villinger, P.J. Santangelo, Visualization of early events in mRNA vaccine delivery in non-human primates via PET–CT and near-infrared imaging, Nat. Biomed. Eng. 3 (2019) 371–380, https://doi.org/10.1038/s41551-019-0378-3.
[41] G. Icardi, A. Orsi, A. Ceravolo, F. Ansaldi, Current evidence on intradermal influenza vaccines administered by SoluviaTM licensed micro injection system, Hum. Vaccin. Immunother. 8 (2012) 67–75, https://doi.org/10.4161/hv.8.1.18419.
[42] A. Giesen, D. Gniel, C. Malerczyk, 30 years of rabies vaccination with Rabipur: a summary of clinical data and global experience, Expert Rev. Vaccines. 14 (2015) 351–367, https://doi.org/10.1586/14760584.2015.1011134.
[43] Y. Levin, E. Kochba, I. Hung, R. Kenney, Intradermal vaccination using the novel microneedle device MicronJet600: past, present, and future, Hum. Vaccin. Immunother. 11 (2015) 991–997, https://doi.org/10.1080/21645515.2015.1010871.
[44] A.J. de Jong, M. Kloppenburg, R.E.M. Toes, A. Ioan-Facsinay, Fatty acids, lipid mediators, and T-cell function, Front. Immunol. 5 (2014), https://doi.org/10.3389/fimmu.2014.00483.
[45] U. Radzikowska, A.O. Rinaldi, Z. Çelebi Sözener, D. Karaguzel, M. Wojcik, K. Cypryk, M. Akdis, C.A. Akdis, M. Sokolowska, The influence of dietary fatty acids on immune responses, Nutrients. 11 (2019) 2990, https://doi.org/10.3390/nu11122990.
[46] F.B. Stentz, A.E. Kitabchi, Palmitic acid-induced activation of human T-lymphocytes and aortic endothelial cells with production of insulin receptors, reactive oxygen species, cytokines, and lipid peroxidation, Biochem. Biophys. Res. Commun. 346 (2006) 721–726, https://doi.org/10.1016/j.bbrc.2006.05.159.
[47] N. Pardi, S. Tuyishime, H. Muramatsu, K. Kariko, B.L. Mui, Y.K. Tam, T.D. Madden, M.J. Hope, D. Weissman, Expression kinetics of nucleoside-modified mRNA delivered in lipid nanoparticles to mice by various routes, J. Control. Release 217 (2015) 345–351, https://doi.org/10.1016/j.jconrel.2015.08.007.
[48] K. Netsomboon, A. Bernkop-Schnürch, Mucoadhesive vs. mucopenetrating particulate drug delivery, Eur. J. Pharm. Biopharm. 98 (2016) 76–89, https://doi.org/10.1016/j.ejpb.2015.11.003.
[49] V. Gerdts, S.D. Littel-Hurk, P.J. Griebel, L.A. Babiuk, Use of animal models in the development of human vaccines, Future Microbiol. 2 (2007) 667–675, https://doi.org/10.2217/17460913.2.6.667.
[50] A. Akinc, W. Querbes, S. De, J. Qin, M. Frank-Kamenetsky, K.N. Jayaprakash, M. Jayaraman, K.G. Rajeev, W.L. Cantley, J.R. Dorkin, J.S. Butler, L. Qin, T. Racie, A. Sprague, E. Fava, A. Zeigerer, M.J. Hope, M. Zerial, D.W. Sah, K. Fitzgerald, M. A. Tracy, M. Manoharan, V. Koteliansky, A. de Fougerolles, M.A. Maier, Targeted delivery of RNAi therapeutics with endogenous and exogenous ligand-based mechanisms, Mol. Ther. 18 (2010) 1357–1364, https://doi.org/10.1038/mt.2010.85.
[51] Y. Suzuki, H. Ishihara, Structure, activity and uptake mechanism of siRNA-lipid nanoparticles with an asymmetric ionizable lipid, Int. J. Pharm. 510 (2016) 350–358, https://doi.org/10.1016/j.ijpharm.2016.06.124.
[52] J.L. Goldstein, M.S. Brown, The LDL receptor, Arterioscler. Thromb. Vasc. Biol. 29 (2009) 431–438, https://doi.org/10.1161/ATVBAHA.108.179564.